



Communication

# Bioinspired Design of Alcohol Dehydrogenase@nano TiO<sub>2</sub> Microreactors for Sustainable Cycling of NAD<sup>+</sup>/NADH Coenzyme

Sen Lin <sup>1,2</sup>, Shiyong Sun <sup>1,2,\*</sup> , Ke Wang <sup>1,2</sup>, Kexuan Shen <sup>1</sup>, Biaobiao Ma <sup>1</sup>, Yuquan Ren <sup>1</sup> and Xiaoyu Fan <sup>2</sup>

<sup>1</sup> Key Laboratory of Solid Waste Treatment and Resource Recycle of Ministry of Education, Institute of Non-Metallic Minerals, Southwest University of Science and Technology, Mianyang 621010, China; linsenzxc@163.com (S.L.); wangke066@126.com (K.W.); skx179az@163.com (K.S.); qinqinmabiao@163.com (B.M.); renyuquan0839@163.com (Y.R.)

<sup>2</sup> Low-cost Wastewater Treatment Technology International Sci-Tech Cooperation Base of Sichuan Province, Mianyang 621010, China; 15929421073@163.com

\* Correspondence: shysun@swust.edu.cn; Tel.: +86-816-2419569

Received: 31 December 2017; Accepted: 19 February 2018; Published: 24 February 2018

**Abstract:** The bioinspired design and construction of enzyme@capsule microreactors with specific cell-like functionality has generated tremendous interest in recent years. Inspired by their fascinating complexity, scientists have endeavored to understand the essential aspects of a natural cell and create biomimicking microreactors so as to immobilize enzymes within the hierarchical structure of a microcapsule. In this study, simultaneous encapsulation of alcohol dehydrogenase (ADH) was achieved during the preparation of microcapsules by the Pickering emulsion method using amphiphilic modified TiO<sub>2</sub> nanoparticles (NPs) as building blocks for assembling the photocatalytic microcapsule membrane. The ADH@TiO<sub>2</sub> NP microreactors exhibited dual catalytic functions, i.e., spatially confined enzymatic catalysis and the membrane-associated photocatalytic oxidation under visible light. The sustainable cycling of nicotinamide adenine dinucleotide (NAD) coenzyme between NADH and NAD<sup>+</sup> was realized by enzymatic regeneration of NADH from NAD<sup>+</sup> reduction, and was provided in a form that enabled further photocatalytic oxidation to NAD<sup>+</sup> under visible light. This bioinspired ADH@TiO<sub>2</sub> NP microreactor allowed the linking of a semiconductor mineral-based inorganic photosystem to enzymatic reactions. This is a first step toward the realization of sustainable biological cycling of NAD<sup>+</sup>/NADH coenzyme in synthetic functional microsystems operating under visible light irradiation.

**Keywords:** enzyme encapsulation; bioinspired microreactors; nicotinamide coenzymes cycling; alcohol dehydrogenase; TiO<sub>2</sub> nanoparticles

## 1. Introduction

In recent years, the design and construction of enzyme@capsule microsystems inspired from the fundamental functions of subcellular organelles has attracted significant attention [1–3]. The development of such highly compartmentalized enzymatic microreactors is motivated by a wide range of applications, such as transformation of energy [4–7], understanding the origin of protolife [8–10], and production of bioactive species with membrane-bounded microcompartments [1,3,11,12].

One of the critical components of bioinspired enzyme@capsule microreactors is the microcapsule membrane employed for the encapsulation or immobilization of the enzyme [8,13,14]. One of the most frequently used techniques for the preparation of a microcapsule is the Pickering emulsion approach, by which solid particles are assembled at the oil/water interface to produce stable emulsion

droplets. To date, a great number of diverse microcapsule membranes with hierarchical structures have been developed from individual building blocks [8,13–15]. Recent studies have shown that inorganic microcapsules with a core-shell structure can be prepared from amphiphilic modified nanoparticles (NPs) of amorphous silica [16], mesoporous silica [17],  $\text{Fe}_3\text{O}_4$  [9],  $\text{TiO}_2$  [18],  $\text{TiO}_2/\text{Fe}_3\text{O}_4$  hybrid, or clay particles [8,19].

Nicotinamide adenine dinucleotide (NAD) is a coenzyme found in all living cells that drives a number of enzyme-catalyzed reactions. It exists in two forms, an oxidized and a reduced form, which are abbreviated as  $\text{NAD}^+$  and NADH, respectively [5,20]. Although several reports have addressed the design and construction of artificial microreactors for mimicking the behavior of cellular regeneration or oxidation of NADH, there are relatively few investigations concerning the sustainable cycling of the  $\text{NAD}^+/\text{NADH}$  coenzyme. Notably,  $\text{TiO}_2$  NPs, as efficient semiconducting NPs, have often been used in different forms, e.g., as a free aqueous dispersion [21], nanocomposite [22], or a confined dispersion in microcapsules [5,9,23]. Herein, we have described bioinspired photoresponsive microreactors comprised of encapsulated alcohol dehydrogenase (ADH) and  $\text{TiO}_2$  NP-assembled microcapsule membranes (Figure 1). Our objective was to initiate the key steps towards sustainable coenzyme cycling based on micro-compartmentalized  $\text{ADH}@\text{TiO}_2$  NP microreactors. Consequently, the photoactive membrane and the enzyme confined within the synthetic cell-like microcapsule were integrated together. In this regard, amphiphilic modified  $\text{TiO}_2$  NPs were used as the Pickering stabilizer for the preparation of water-in-oil colloidosomes (microcapsules). ADH was simultaneously encapsulated into the  $\text{TiO}_2$  NP-stabilized microcapsules during the preparation of water-in-oil Pickering emulsion droplets. The as-prepared water-in-water  $\text{ADH}@\text{TiO}_2$  NP microreactors were modified with a layer of polydopamine (PDA) to enhance the utilization of visible light. PDA was formed by the polymerization of dopamine (DA) after being cross-linked and transferred into the aqueous phase. Specifically, we initiated the spatially confined enzyme reaction within a population of  $\text{ADH}@\text{TiO}_2$  NP microreactors to generate NADH from  $\text{NAD}^+$  reduction, which diffused through the medium and induced subsequent membrane-associated photocatalytic oxidation to produce  $\text{NAD}^+$  under visible light irradiation. During the reduction process, the ethanol in the reaction system lost a hydrogen atom under the catalytic action of ADH within the microreactors, and subsequently, the  $\text{NAD}^+$  gained this free hydrogen atom and was reduced to NADH. Under visible light irradiation, NADH was catalytically oxidized to  $\text{NAD}^+$  by the PDA-modified  $\text{TiO}_2$  NP membrane on the surface of the microreactors. Subsequently, the oxidized  $\text{NAD}^+$  regenerated NADH again in the dehydrogenation reaction catalyzed by the ADH and newly added ethanol. Thus, the sustainable cycling of  $\text{NAD}^+/\text{NADH}$  coenzyme was realized by using  $\text{ADH}@\text{TiO}_2$  NP microreactors.

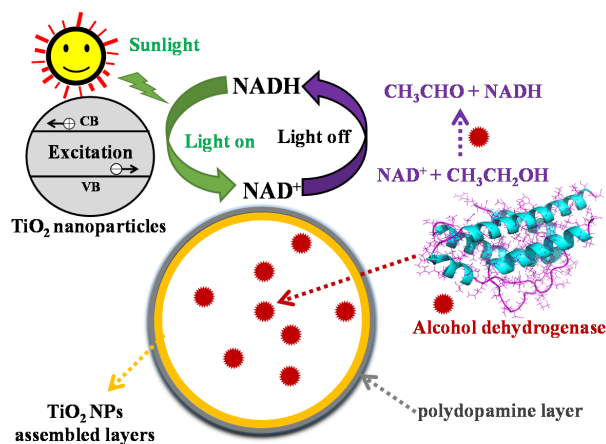


**Figure 1.** Schematic illustration of the cycling of nicotinamide coenzymes  $\text{NAD}^+/\text{NADH}$  catalyzed by the bioinspired  $\text{ADH}@\text{TiO}_2$  NP microreactors. The polydopamine layer was formed by means of in situ polymerization of dopamine and used as a photosensitizer for the activation of the  $\text{TiO}_2$  NP membrane under visible light. During cycling of  $\text{NAD}^+/\text{NADH}$ , enzymatic regeneration of NADH from  $\text{NAD}^+$  reduction is catalyzed by alcohol dehydrogenase and subsequent photocatalytic oxidation to  $\text{NAD}^+$  takes place by the PDA-modified  $\text{TiO}_2$  NP membrane under visible light irradiation.

## 2. Materials and Methods

### 2.1. Materials

Commercial 3-aminopropyltriethoxysilane (APTES)-modified TiO<sub>2</sub> NPs (TiO<sub>2</sub> content  $\geq$  95%) were purchased from Huizhe Fine Chemistry Co., Ltd. (Suzhou, China). Hexamethylene tetramine (HMTA, purity  $\geq$  99.5%) and hydrogen peroxide (purity 30%) were obtained from Aladdin Biochemical Technology Co., Ltd. (Shanghai, China). DA (purity  $\geq$  98%), NAD<sup>+</sup> (purity  $\geq$  98%), NADH (purity  $\geq$  98%), Fluorescein isothiocyanate (FITC) and ADH were purchased from Hefei Bomei Biological Technology Co., Ltd. (Hefei, China). Ethanol, toluene, tetraethoxysilane (TEOS) and Tris-HCl were purchased from Chengdu Kelong Chemical Reagent Factory (Chengdu, China). All other chemicals were of analytical grade and used without further purification. All water used in experiments was obtained from Millipore water purification system Milli-Q Integral 5 (Paris, France) (resistance  $\geq$  18.25 M $\Omega$ ·cm<sup>-1</sup>).

### 2.2. Preparation of PDA-Modified ADH@TiO<sub>2</sub> NP Microreactors

The ADH@TiO<sub>2</sub> NP water-in-oil microcapsules (microreactors) were prepared by the Pickering emulsion method [8]. A calculated amount of TiO<sub>2</sub> (10 mg) was dispersed in 10 mL of toluene and sonicated in an ultrasonic bath for 15 min. Typically, an aqueous solution containing 200  $\mu$ L of ADH or FITC-labeled ADH (FITC-ADH) (100 U·mL<sup>-1</sup>) was added to 2 mL toluene containing 1 mg·mL<sup>-1</sup> TiO<sub>2</sub> dispersion. The mixture was homogenized for 1 min using a homogenizer (F10, Fluko, Berlin, Germany) at 10,000 rpm. Subsequently, the surface of the water-in-oil microcapsules was cross-linked by hydrolytic reaction with 70  $\mu$ L of TEOS for 24 h. The water-in-water ADH@TiO<sub>2</sub> NP microreactors were prepared after toluene was removed by ethanol washing and transferred into the continuous water phase.

The surface of the ADH@TiO<sub>2</sub> NP microreactors was modified with PDA, which was formed by the polymerization of dopamine under alkaline conditions, in order to improve their photocatalytic activity [19]. The ADH@TiO<sub>2</sub> NP microreactors were incubated with 2 mL of 0.2 mg·mL<sup>-1</sup> DA aqueous solution. Then, 4 mg of HMTA was added to the suspension to induce the formation of the PDA layer on the surface of the microcapsules under the weakly alkaline environment. The PDA-coated ADH@TiO<sub>2</sub> NP microreactors were isolated by centrifugation of the reaction mixture at 8000 rpm for 5 min. The ADH@TiO<sub>2</sub> NP microreactors were washed thrice with ethanol.

### 2.3. NAD<sup>+</sup>/NADH Cycling Catalyzed by ADH@TiO<sub>2</sub> NP Microreactors

First, 1 mM NAD<sup>+</sup> and 1 mM NADH solutions were prepared in a buffer (100 mM Tris-HCl and 10 mM sodium phosphate, pH 7.5). In a typical NADH generation procedure, 300  $\mu$ L of the NAD<sup>+</sup> solution and 1.6 mL of the buffer solution were added into 0.01 mg·mL<sup>-1</sup> dispersion of the ADH@TiO<sub>2</sub> NP microreactors. Then, 100  $\mu$ L of ethanol (concentration was 50%) was added to the mixture to initiate the enzymatic reaction at 37 °C. The concentration of generated NADH was determined by monitoring the increasing intensity of the UV-visible absorption band at 340 nm at given time intervals using a micro-spectrophotometer with an integrated normal cuvette (Nanodrop 2000C, Thermo, Shanghai, China). For the oxidation of NADH, the reaction mixture was placed into a quartz reactor equipped with a stirring bar. The visible light irradiation source was a 300 W Xenon lamp (AuLight CEL-HXF300, Beijing, China) with a cut-off filter of 420 nm. The visible light intensity in the photocatalytic test section was 1300 mW·cm<sup>-2</sup>. The distance between the reactor and the light lamp was fixed at 5 cm. During the experiment, the concentration of NAD<sup>+</sup> was estimated by measuring the decreasing absorption at 340 nm. Finally, another 100  $\mu$ L of ethanol was added to the reaction system to initiate the regeneration of NADH at 37 °C without light illumination. The cycling of NAD<sup>+</sup>/NADH was evaluated more than 20 times.

#### 2.4. Characterization

The morphology of the prepared microcapsules was observed by an optical microscope (DM 2000, Leica, Bonn, Germany), scanning electron microscope (SEM, Ultra 55, Zeiss, Berlin, German), and transmission electron microscope (TEM, Libra 200, Zeiss, Berlin, Germany). The microreactors were also characterized by Fourier transform infrared (FT-IR) spectroscopy using a Spectrum One (American PE, Cincinnati, OH, USA) spectrometer. The UV-Vis absorption spectra were recorded on an ultraviolet solid diffuse reflectometer (UV-DRS, UV-3150, Shimadzu, Kyoto, Japan). The particle size distribution of the tourmaline particles was characterized by a particle size analyzer (Plus 90, Brookhaven, Holtsville, NY, USA). The mineral phase of tourmaline was characterized by an X-ray diffractometer (X'pert Pro, PANalytical, Eindhoven, The Netherlands). Confocal laser scanning microscopy (CLSM) images of the distributions of FITC-labeled ADH within the microcapsules were obtained on an inverted CLSM (TCS SP8, Leica, Mannheim, Germany).

### 3. Results and Discussion

The water-in-oil Pickering emulsion microcapsules were prepared by using amphiphilic TiO<sub>2</sub> NPs as a stabilizer at the water-toluene interface. APTES is an aminosilane that is frequently used in the process of amphiphilic surface modification of nanoparticles. Therefore, APTES-grafted TiO<sub>2</sub> NPs were used in the experiments as the Pickering stabilizer. The APTES-modified TiO<sub>2</sub> NPs were in anatase phase with an average diameter of ~74 nm and contact angle of ~83.7° (see details in Figures S1–S4, Supporting Information). The resulting water-in-oil emulsion microcapsules were prepared after the TiO<sub>2</sub> NPs assembled at the oil-water interface. Optical microscopy images showed discrete spherical microcapsules (Figure 2a and Figure S5, Supporting Information). The microcapsule membrane was cross-linked by the TEOS hydrolysis reaction to stabilize the structural integrity after being transferred to the aqueous phase (Figure 2b) [8,19]. SEM images showed that the dried microcapsules had distinctive TiO<sub>2</sub> NP layers with rough surfaces Figure 2c,d,f. ADH was simultaneously encapsulated into the TiO<sub>2</sub> NPs microcapsules and assembled into ADH@TiO<sub>2</sub> NP microreactors. CLSM observations of the fluorescent FITC-labeled membranes confirmed that ADH was well-encapsulated into the TiO<sub>2</sub> NP membranes (Figure 2e). The ADH@TiO<sub>2</sub> NP microreactors exhibited size polydispersity, which was dependent on the water/TiO<sub>2</sub> volume/weight ratio used in the preparations. The mean diameter varied from ~60 to 110 μm with ratios ranging from 50 to 250 μL·mg<sup>-1</sup> (Figure 2g and Figure S6, Supporting Information).

TiO<sub>2</sub> is a well-known n-type semiconductor that has long been used for photocatalysis [5,21–23]. However, pristine TiO<sub>2</sub> NPs with a band gap larger than 3.0 eV are only active under ultra-violet light illumination [24]. To utilize a wider solar spectrum of visible light and enable visible light photoactivation of pristine TiO<sub>2</sub> NPs, modification with PDA is an effective strategy, and is achieved by the in situ polymerization of dopamine onto the surface of the microcapsules [24]. Therefore, PDA surface modification of ADH@TiO<sub>2</sub> NP microreactors was also performed in our study. The pristine TiO<sub>2</sub> NPs show absorption only in the UV region without any detectable absorption of visible light (Figure S6, Supporting Information). In contrast, the UV-Vis adsorption spectrum of PDA-modified ADH@TiO<sub>2</sub> NP microreactors indicated significant visible light absorption, suggesting that the solar energy conversion efficiency was enhanced after PDA surface modification (Figure S6, Supporting Information). FT-IR spectra of the ADH@TiO<sub>2</sub> NP microreactors showed characteristic peaks of TiO<sub>2</sub> NPs, ADH, and PDA, suggesting the coexistence of encapsulated ADH, PDA, and TiO<sub>2</sub> NP microcapsule membranes (Figure S7, Supporting Information).

The enzymatic activity of free ADH and visible light-driven photocatalysis of TiO<sub>2</sub> NPs microcapsules without ADH were separately evaluated. The reaction dispersions were exposed to either a 5000 lux visible light source or placed in the dark with the addition of ethanol. The concentration of NADH was calculated by the absorption intensity of its characteristic peak at 340 nm (Figure S8, Supporting Information) [18]. The formation of NADH was catalyzed by free ADH and monitored by the increase in the absorption at 340 nm Figure 3a,b. Conversely, the generation



of  $\text{NAD}^+$  from the oxidation of NADH under visible light in the reaction mixture was estimated by the decreasing intensity of NADH Figure 3c,d. Normally, both free ADH and  $\text{TiO}_2$  NP microcapsules without ADH presented their own catalytic performances Figure 3.

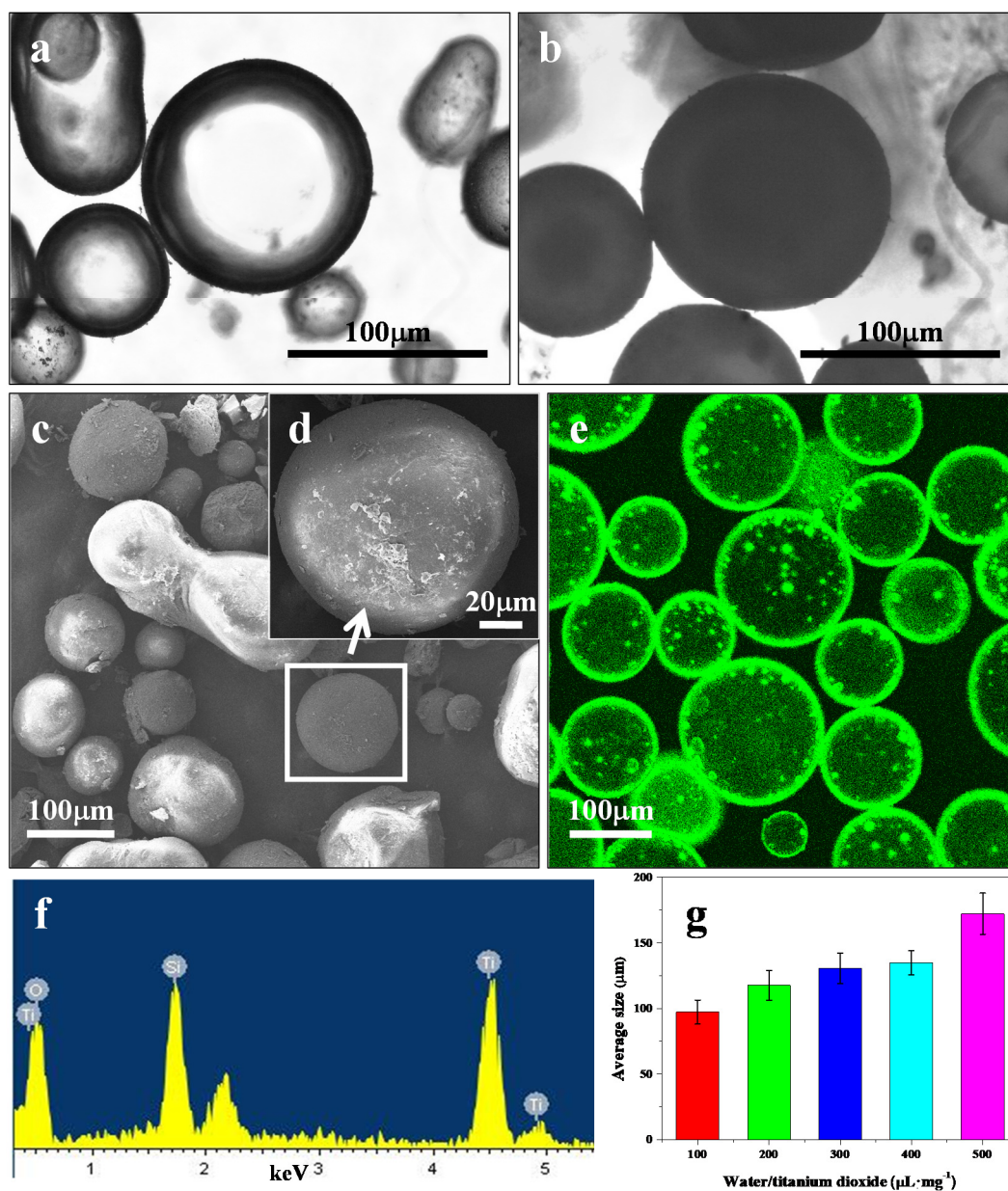


**Figure 2.** Microscopic images of the ADH@ $\text{TiO}_2$  NP microreactors. (a,b) Optical images; (c,d) SEM images; and (e) CLSM image. (a) Water-in-oil Pickering emulsions before being cross-linked by TEOS; (b) Water-in-water microcapsules after being cross-linked by TEOS; (c,d) SEM images of the dried ADH@ $\text{TiO}_2$  NP microreactors; (e) CLSM image of the FITC labeled ADH@ $\text{TiO}_2$  NP microreactors; (f) EDS analysis of the ADH@ $\text{TiO}_2$  NP microreactors; (g) Average size distributions, median values, and standard deviations were calculated by fitting Gaussian functions to the histograms.

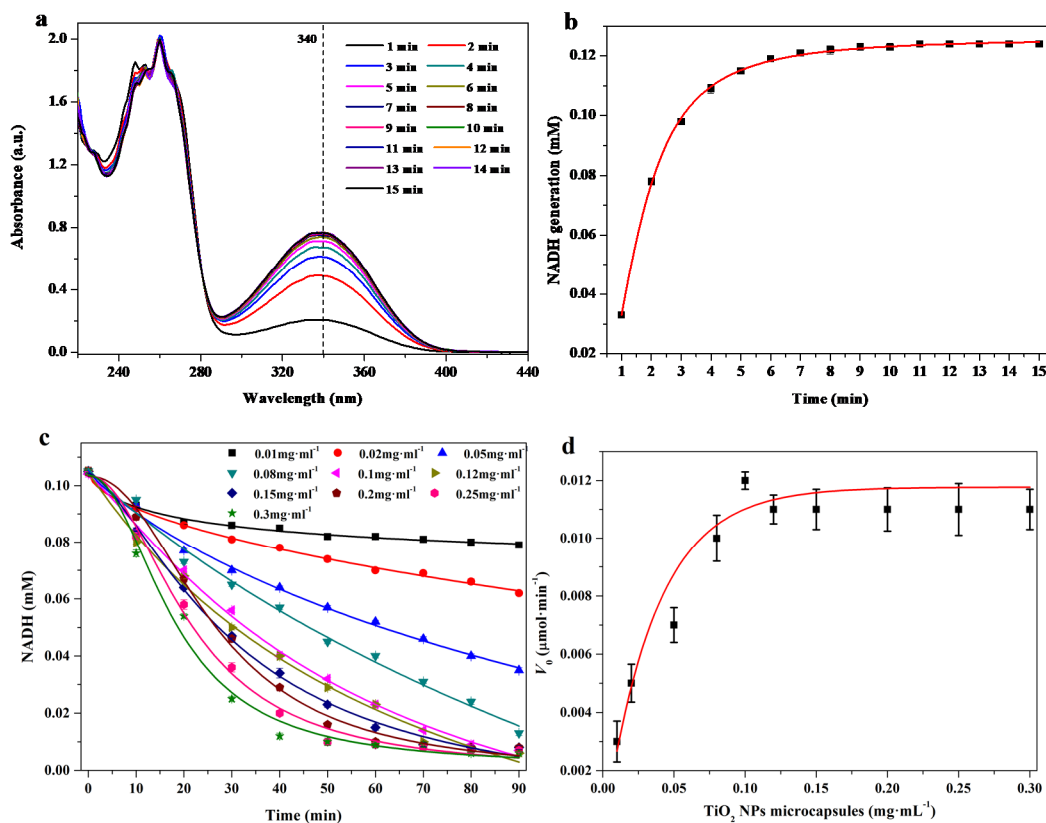


**Figure 3.** UV-Vis spectra showing that the increase in absorption intensity at 340 nm is consistent with the reduction of  $\text{NAD}^+$  to  $\text{NADH}$  in a reaction mixture containing  $\text{NAD}^+$  (1 mM, 300  $\mu\text{L}$ ), ethanol (50%, 100  $\mu\text{L}$ ), and ADH (10  $\mu\text{g}\cdot\text{mL}^{-1}$ , 100  $\mu\text{L}$ ) at 37 °C and pH 7.5. (a) Corresponding plots of intensity at 340 nm vs. time; (b) Plots of  $\text{NADH}$  concentration vs. time. UV-Vis absorption intensity at 340 nm was consistent with the oxidation of  $\text{NADH}$  to  $\text{NAD}^+$  under visible light irradiation in a reaction mixture containing  $\text{NADH}$  (1 mM, 200  $\mu\text{L}$ ),  $\text{TiO}_2$  NP microcapsules without ADH and with varying  $\text{TiO}_2$  NP microcapsules concentrations from 0.01 to 0.3  $\text{mg}\cdot\text{mL}^{-1}$  at 37 °C and pH 7.5; (c) Corresponding plots of  $\text{NADH}$  concentration decreasing vs. time; (d) Initial velocity ( $V_0$ ) vs. concentration of the microcapsules.

The cycling performance of  $\text{NAD}^+$  and  $\text{NADH}$  catalyzed by  $\text{ADH@TiO}_2$  NP microreactors is shown in Figure 4. In the first step of a typical cycling of  $\text{NADH}$  generation- $\text{NADH}$  oxidation to  $\text{NAD}^+$ - $\text{NADH}$  regeneration,  $\text{NAD}^+$  was catalytically reduced to  $\text{NADH}$  by the spatially confined ADH. In the second step of cycling,  $\text{NADH}$  oxidation in reaction system was initialized upon exposure to visible light irradiation (Figure 4b). To complete the cycle,  $\text{NADH}$  was regenerated by the addition of ethanol to switch on the ADH function for the reduction of  $\text{NAD}^+$  to  $\text{NADH}$  without visible light illumination (Figure 4c). According to the experimental results (Figure 4a–c), sustainable biological cycling of  $\text{NAD}^+$ / $\text{NADH}$  coenzyme was realized in the synthetic functional microreactors under visible light irradiation. The catalytic stability of the  $\text{ADH@TiO}_2$  NP microreactors was also investigated (Figure 4d). The results indicated that the  $\text{ADH@TiO}_2$  NP microreactors were sufficiently stable even after 13 consecutive cycles.

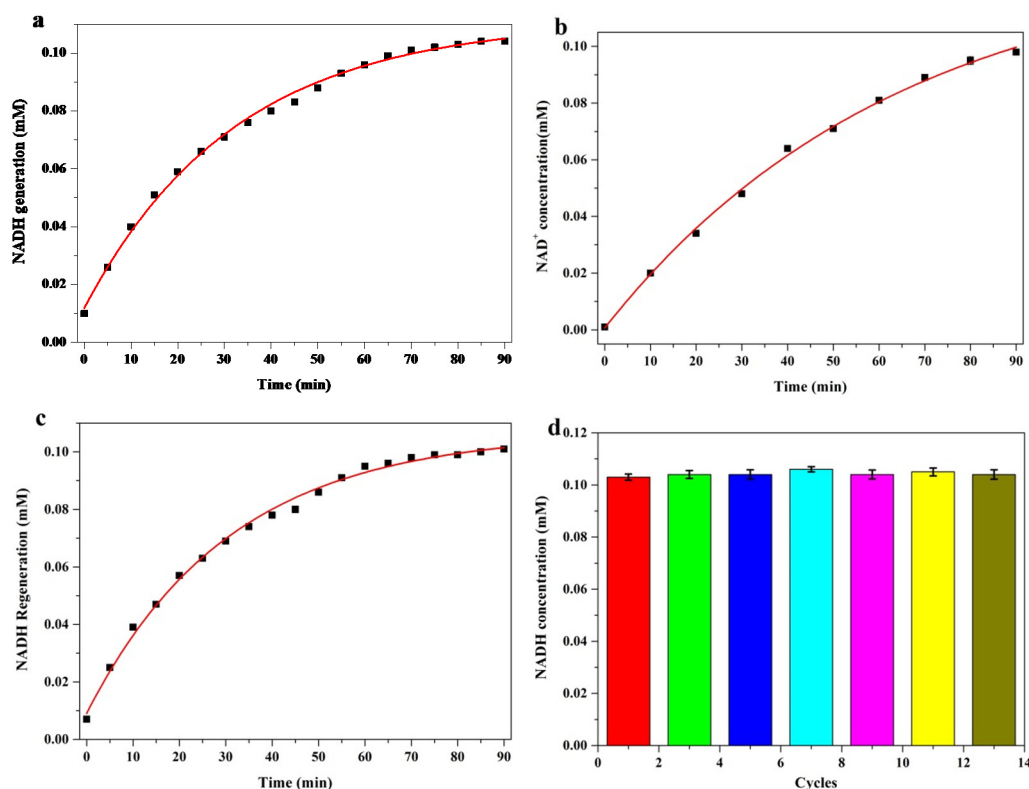


**Figure 4.** NAD<sup>+</sup>/NADH cycling performance catalyzed by ADH@TiO<sub>2</sub> NP microreactors. (a) Reduction of NAD<sup>+</sup> to NADH; (b) Oxidation of NADH to NAD<sup>+</sup> under visible light irradiation; (c) Regeneration of NADH from oxidized NAD<sup>+</sup>; (d) Cycling performance in 13 cycles. A reduction reaction mixture containing ADH@TiO<sub>2</sub> NP microreactors (0.1 mg·mL<sup>-1</sup>), NAD<sup>+</sup> (1 mM, 300 μL), and ethanol (50%, 100 μL) at 37 °C and pH 7.5.

#### 4. Conclusions

In summary, novel bioinspired photoresponsive ADH@TiO<sub>2</sub> NP microreactors were developed to facilitate the mimicking of sustainable nicotinamide coenzymes of NAD<sup>+</sup>/NADH cycling in a synthetic functional microcompartment under visible light irradiation. The designed microreactors represent a model of a simple nonbiological microsystem that is related to enzymatic catalysis and inorganic photochemical reactions. Thus, our research provides new opportunities in visible light energy capture and transduction. Furthermore, it is possible to synthesize this simple microsystem easily and on a large scale. Consequently, the proposed membrane-bounded microcompartments with core-shell hierarchical structure have great potential in photoactive microreactor design and drug delivery.

**Supplementary Materials:** The following are available online at <http://www.mdpi.com/2079-4991/8/2/127/s1>, Figure S1: X-ray diffraction pattern of 3-aminopropyltriethoxysilane (APTES) modified TiO<sub>2</sub> NPs, Figure S2: Transmission electron microscope (TEM) characterization of APTES modified TiO<sub>2</sub> NPs. TEM images (a,b), Figure S3: Size distribution of APTES modified TiO<sub>2</sub> NPs. The average particle size is ca. 74 nm, Figure S4: Photographs of water droplets mounted on the surface of TiO<sub>2</sub> NPs showing stable droplets on APTES modified TiO<sub>2</sub> NPs due to amphiphilic character (a); and droplet spreading on conventional hydrophilic P25-type TiO<sub>2</sub> NPs (b), respectively. The corresponding mean contact angle for droplets on APTES modified TiO<sub>2</sub> NPs was ca. 83.7°, Figure S5: Size distribution of ADH@TiO<sub>2</sub> NPs microreactors with water/TiO<sub>2</sub> volume/weight ratio from 50 μL·mg<sup>-1</sup> (a); 100 μL·mg<sup>-1</sup> (b); 150 μL·mg<sup>-1</sup> (c); 200 μL·mg<sup>-1</sup> (d) and 250 μL·mg<sup>-1</sup> (e), Figure S6: UV-Vis adsorption spectral characterization of TiO<sub>2</sub> NPs, PDA and PDA modified ADH@TiO<sub>2</sub> NPs microreactors with varied concentrations from 0.1 to 1 mg·mL<sup>-1</sup>, Figure S7: FTIR spectral characterization of TiO<sub>2</sub> NPs, PDA and PDA modified ADH@TiO<sub>2</sub> NPs microreactors with varied concentrations from 0.1 to 0.6 mg·mL<sup>-1</sup>, Figure S8: Chemical formula (a) and UV-Vis spectra (b) of NAD<sup>+</sup> and NADH.

**Acknowledgments:** The present work was partly supported by the National Natural Science Foundation of China (41672039), National Basic Research Program of China (973 Program: 2014CB846003), The Longshan Academic

Talent Research Support Program of the Southwest University of Science and Technology (17LZX419, 17LZXT05), and Postgraduate Innovation Fund Project of Southwest University of Science and Technology (17ycx044).

**Author Contributions:** Shiyong Sun contributed to design experiments. Sen Lin, Ke Wang, Kexuan Shen and Biaobiao Ma performed experiments. The initial manuscript draft was written by Sen Lin and further improved by Shiyong Sun, Yuquan Ren and Xiaoyu Fan.

**Conflicts of Interest:** The authors declare no conflict of interest.

## References

1. Miller, D.M.; Gulbis, J.M. Engineering protocells: Prospects for self-assembly and nanoscale production-lines. *Life* **2015**, *5*, 1019–1053. [[CrossRef](#)] [[PubMed](#)]
2. Yin, Y.; Lin, N.; Zhu, X.; Zhao, M.; Zhang, Z.; Mann, S.; Liang, D. Non-equilibrium behaviour in coacervate-based protocells under electric-field-induced excitation. *Nat. Commun.* **2016**, *7*, 10658. [[CrossRef](#)] [[PubMed](#)]
3. Buddingh, B.C.; van Hest, J.C.M. Artificial cells: Synthetic compartments with life-like functionality and adaptivity. *Acc. Chem. Res.* **2017**, *50*, 769–777. [[CrossRef](#)] [[PubMed](#)]
4. Marpani, F.; Pinelo, M.; Meyer, A.S. Enzymatic conversion of CO<sub>2</sub> to CH<sub>3</sub>OH via reverse dehydrogenase cascade biocatalysis: Quantitative comparison of efficiencies of immobilized enzyme systems. *Biochem. Eng. J.* **2017**, *127*, 217–228. [[CrossRef](#)]
5. Summers, D.P.; Rodoni, D. Vesicle encapsulation of a nonbiological photochemical system capable of reducing NAD<sup>+</sup> to NADH. *Langmuir* **2015**, *31*, 10633–10637. [[CrossRef](#)] [[PubMed](#)]
6. Jiang, B.B.; Wang, X.D.; Wu, D.Z. Fabrication of microencapsulated phase change materials with TiO<sub>2</sub>/Fe<sub>3</sub>O<sub>4</sub> hybrid shell as thermoregulatory enzyme carriers: A novel design of applied energy microsystem for bioapplications. *Appl. Energy* **2017**, *201*, 20–33. [[CrossRef](#)]
7. Li, J.D.; Liu, H.; Wang, X.D.; Wu, D.Z. Development of thermoregulatory enzyme carriers based on microencapsulated *N*-docosane phase change material for biocatalytic enhancement of amylases. *ACS Sustain. Chem. Eng.* **2017**, *5*, 8396–8406. [[CrossRef](#)]
8. Sun, S.; Li, M.; Dong, F.; Wang, S.; Tian, L.; Mann, S. Chemical signaling and functional activation in colloidosome-based protocells. *Small* **2016**, *12*, 1920–1927. [[CrossRef](#)] [[PubMed](#)]
9. Rodriguez-Arco, L.; Li, M.; Mann, S. Phagocytosis-inspired behaviour in synthetic protocell communities of compartmentalized colloidal objects. *Nat. Mater.* **2017**, *16*, 857–863. [[CrossRef](#)] [[PubMed](#)]
10. Akkarachaneeyakorn, K.; Li, M.; Davis, S.A.; Mann, S. Secretion and Reversible Assembly of Extracellular-like Matrix by Enzyme-Active Colloidosome-Based Protocells. *Langmuir* **2016**, *32*, 2912–2919. [[CrossRef](#)] [[PubMed](#)]
11. Zhang, S.; Jiang, Z.; Zhang, W.; Wang, X.; Shi, J. Polymer–inorganic microcapsules fabricated by combining biomimetic adhesion and bioinspired mineralization and their use for catalase immobilization. *Biochem. Eng. J.* **2015**, *93*, 281–288. [[CrossRef](#)]
12. Wang, J.; Huang, R.; Qi, W.; Su, R.; He, Z. Oriented enzyme immobilization at the oil/water interface enhances catalytic activity and recyclability in a pickering emulsion. *Langmuir* **2017**, *33*, 12317–12325. [[CrossRef](#)] [[PubMed](#)]
13. Hassan, M.M.; Atiqullah, M.; Beg, S.A.; Chowdhury, M.H.M. Effects of enzyme microcapsule shape on the performance of a nonisothermal packed-bed tubular reactor. *J. Chem. Technol. Biot.* **2015**, *66*, 41–55. [[CrossRef](#)]
14. Zheng, Z.; Jin, J.; Xu, G.K.; Zou, J.; Wais, U.; Beckett, A.; Heil, T.; Higgins, S.; Guan, L.; Wang, Y. Highly stable and conductive microcapsules for enhancement of joule heating performance. *ACS Nano* **2016**, *10*, 4695–4703. [[CrossRef](#)] [[PubMed](#)]
15. Li, Y.L.; Zhu, M.L.; Li, X.Y.; Li, X.H.; Jiang, Y. A highly expandable and tough polyacrylamide–alginate microcapsule. *Rsc Adv.* **2016**, *6*, 44896–44901. [[CrossRef](#)]
16. Wang, S.; Li, M.; Patil, A.J.; Sun, S.; Tian, L.; Zhang, D.; Cao, M.; Mann, S. Design and construction of artificial photoresponsive protocells capable of converting day light to chemical energy. *J. Mater. Chem. A* **2017**, *5*, 24612–24616. [[CrossRef](#)]



17. Huo, C.; Li, M.; Huang, X.; Yang, H.; Mann, S. Membrane engineering of colloidosome microcompartments using partially hydrophobic mesoporous silica nanoparticles. *Langmuir* **2014**, *30*, 15047–15052. [[CrossRef](#)] [[PubMed](#)]
18. Chen, T.; Colver, P.J.; Bon, S.A.F. Organic-inorganic hybrid hollow spheres prepared from TiO<sub>2</sub>-stabilized pickering emulsion polymerization. *Adv. Mater.* **2007**, *19*, 2286–2289. [[CrossRef](#)]
19. Lin, S.; Sun, S.; Shen, K.; Tan, D.; Zhang, H.; Dong, F.; Fu, X. Photocatalytic microreactors based on nano TiO<sub>2</sub>-containing clay colloidosomes. *Appl. Clay Sci.* **2017**. [[CrossRef](#)]
20. Uppada, V.; Bhaduri, S.; Noronha, S.B. Cofactor regeneration—an important aspect of biocatalysis. *Curr. Sci.* **2014**, *106*, 946–957.
21. Jin, B.; Yao, G.; Wang, X.; Ding, K.; Jin, F. Photocatalytic oxidation of glucose into formate on nano TiO<sub>2</sub> catalyst. *ACS Sustain. Chem. Eng.* **2017**, *5*, 6377–6381. [[CrossRef](#)]
22. Sun, H.; Peng, T.; Liu, B.; Xian, H. Effects of montmorillonite on phase transition and size of TiO<sub>2</sub> nanoparticles in TiO<sub>2</sub>/montmorillonite nanocomposites. *Appl. Clay Sci.* **2015**, *114*, 440–446. [[CrossRef](#)]
23. Lv, K.; Perriman, A.W.; Mann, S. Photocatalytic multiphase micro-droplet reactors based on complex coacervation. *Chem. Commun.* **2015**, *51*, 8600–8602. [[CrossRef](#)] [[PubMed](#)]
24. Mao, W.; Lin, X.; Zhang, W.; Chi, Z.; Lyu, R.; Cao, A.; Wan, L. Core-shell structured TiO<sub>2</sub>@polydopamine for highly active visible-light photocatalysis. *Chem. Commun.* **2016**, *52*, 7122–7125. [[CrossRef](#)] [[PubMed](#)]



© 2018 by the authors. Licensee MDPI, Basel, Switzerland. This article is an open access article distributed under the terms and conditions of the Creative Commons Attribution (CC BY) license (<http://creativecommons.org/licenses/by/4.0/>).